# Conformational flexibility and molecular dynamics of cationic diolefin–rhodium(I) complexes with iminophosphine ligands

Bruno Crociani *, Simonetta Antonaroli, Maria Luisa Di Vona, Silvia Licoccia

*Dipartimento di Scienze e Tecnologie Chimiche, Universita' di Roma Tor Vergata, Via della Ricerca Scientifica 1, 00133 Rome, Italy*

## Abstract

In solution, the cationic complexes $[Rh(\eta^2,\eta^2\text{-diolefin})(P–N)]^+$ [diolefin = 1,5-cyclooctadiene (cod), bicyclo[2.2.1]hepta-2,5-diene (nbd); P–N = $o$-(PPh$_2$)C$_6$H$_4$CH=NR (R = C$_6$H$_3$($i$-Pr)$_2$-2,6 (**1**), CMe$_3$ (**2**), (R)-bornyl (**3**)] undergo a conformational change of the iminophosphine ligand which inverts the position of the six-membered chelate ring relative to the N–Rh–P coordination plane. The inversion is fast for $[Rh(\eta^2,\eta^2\text{-diolefin})(\mathbf{1})]^+$ and $[Rh(\eta^2,\eta^2\text{-diolefin})(\mathbf{3})]^+$ in the temperature range 298–183 K, and becomes progressively slower for $[Rh(\eta^2,\eta^2\text{-diolefin})(\mathbf{2})]^+$ with increasing steric demand of the coordinated ligands. From the coalescing signals in the $^1$H-NMR spectrum of $[Rh(nbd)(\mathbf{2})]^+$ at 208 K, a $\Delta H^{\#}$ value of 28.5 kJ mol$^{-1}$ and a $\Delta S^{\#}$ value of $-60.3$ J K$^{-1}$ mol$^{-1}$ can be estimated. The phase-sensitive 2D $^1$H-NMR ROESY spectrum of $[Rh(cod)(\mathbf{3})]^+$ reveals the presence of another dynamic process which slowly and selectively interconverts the two olefinic protons on the same HC=CH unit of the chelate diolefin. A mechanism is proposed involving the initial dissociation of the rhodium–olefin bond *trans* to phosphorus. Semi-empirical calculations show that in the most stable conformers of $[Rh(nbd)(\mathbf{2})]^+$ and $[Rh(cod)(\mathbf{2})]^+$ the P–N chelate ring is not coplanar with the N–Rh–P plane, while the diolefin coordination mode is distorted largely by the steric interaction with the bulky N–CMe$_3$ group. When the P–N chelate ring is forced to be coplanar with the N–Rh–P plane, the enthalpy content increases to 20.3 and 114.7 kJ mol$^{-1}$ for $[Rh(nbd)(\mathbf{2})]^+$ and $[Rh(cod)(\mathbf{2})]^+$, respectively. Entropy factors seem to be predominant in the displacement of 1,5-cyclooctadiene by other olefinic ligands in the complexes $[Rh(cod)(P–N)]^+$. © 2001 Elsevier Science B.V. All rights reserved.

*Keywords:* Solution dynamics; $[Rh(\eta^2,\eta^2\text{-diolefin})(\text{iminophosphine})]^+$; 2D-exchange NMR; Semi-empirical calculations

## 1. Introduction

Recently, palladium complexes with iminophosphine ligands such as N-[(2-diphenylphosphino)benzylidene]-amines (P–N) have been employed successfully as catalysts (or catalysts precursors) in the cross-coupling of aryl halides with organostannanes [1], carbostannylation of alkynes [1], oligomerisation of ethene [2], CO/olefin copolymerisation [3], and asymmetric allylic alkylation [4]. From X-ray structural studies on palladium(II) and palladium(0) derivatives it appears that the six-membered chelate ring formed by the P,N-bonded iminophosphine is not coplanar with the N–Pd–P coor-

dination plane [5]. In solution, however, the P–N ligands undergo a low-energy conformational change involving the inversion of the chelate ring, whereby the phosphine phenyl groups interchange their positions, while the N-substituent and the –C$_6$H$_4$CH= unit move above and below the N–Pd–P plane [5].

Rhodium(I) complexes with P,N-donor bidentate ligands have also been used in the catalytic hydroformylation [6] and asymmetric hydroboration [7] of olefins, as well as in the catalytic hydrogenation of arenes [8].

In order to verify that conformational rearrangements similar to those observed in palladium derivatives would occur also in rhodium complexes and to get more information about the influence of steric factors on such processes, we have studied the solution behaviour of a series of cationic $\eta^2,\eta^2$-diolefin–rhodium(I) complexes with iminophosphines carrying bulky N-substituents. A better understanding of the molecular

dynamics of these compounds is a prerequisite for their application in catalysis.

## 2. Results and discussion

### 2.1. Preparation and characterisation of the complexes

The complexes $[Rh(\eta^2,\eta^2\text{-diolefin})(P–N)]BF_4$ [diolefin = 1,5-cyclooctadiene (cod), norbornadiene (nbd); P–N = $o$-(Ph$_2$P)C$_6$H$_4$CH=NR] are obtained readily from the reaction of $[Rh(\eta^2,\eta^2\text{-diolefin})_2]BF_4$ with the appropriate iminophosphine (Eq. (1) of Scheme 1). Anhydrous solvents are required generally since the products decompose slowly if trace amounts of water are present in solution. A P–N/Rh molar ratio of 1:1 is also required because an excess of iminophosphine leads to the formation of the cationic species $[Rh(P–N)_2]^+$, identified by the characteristic $^{31}$P-NMR resonances in the range 55–51 ppm [9].
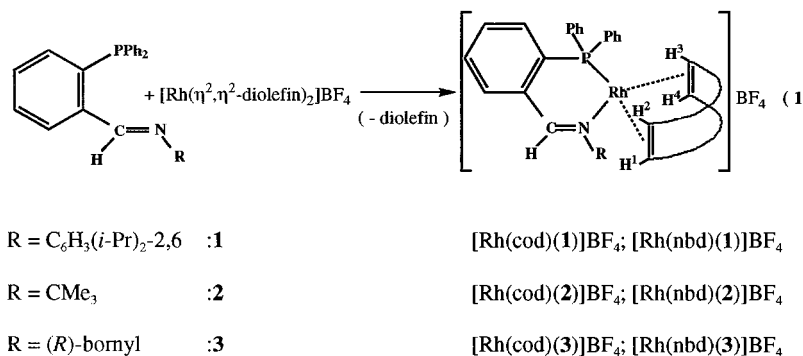
Only the complex $[Rh(cod)(3)]^+$ appears to be sufficiently stable, even in the presence of water, as to be isolated as perchlorate salt from the reaction of $[Rh(\mu\text{-Cl})(cod)]_2$ with ligand **3** and NaClO$_4$·H$_2$O in commercial grade solvents. All the new compounds have been characterised by elemental analysis, IR spectra, conductivity measurements (see Section 3), and by $^1$H- and $^{31}$P{$^1$H}-NMR spectroscopy. Some selected NMR data are listed in Table 1.

The upfield shift of the N=CH signals and the downfield shift of the $^{31}$P resonances relative to the free ligands [10] clearly indicate that the iminophosphines are P,N-bound to the metal centre. The phosphorus coordination is further confirmed by the $^{103}$Rh–$^{31}$P coupling constants in the range 152.9–155.1 and 170.2–170.5 Hz for the 1,5-cyclooctadiene and norbornadiene derivatives, respectively, which are typical for square-planar complexes $[Rh(\eta^2,\eta^2\text{-diolefin})(L–L')]^+$

(L–L' = P,N-bidentate ligands) [11]. Two sets of olefinic proton resonances are observed: one at lower field assigned to the H$^1$ and H$^2$ protons *trans* to P, and the other at higher field assigned to the H$^3$ and H$^4$ protons *trans* to N, in agreement with literature data [11,12]. This assignment is supported strongly by the interligand NOEs in the 2D $^1$H-NMR ROESY spectra of $[Rh(cod)(3)]^+$ (discussed later).

### 2.2. Dynamic behaviour in solution

The solution behaviour of the tetrafluoborate salts has been studied by $^1$H-NMR spectra at different temperatures in CD$_2$Cl$_2$ and also by 2D $^1$H-NMR ROESY experiments for $[Rh(cod)(3)]BF_4$ and $[Rh(cod)(3)]ClO_4$ in both CD$_2$Cl$_2$ and CDCl$_3$ solvents. The spectral features observed suggest that all the cationic derivatives are fluxional. For $[Rh(cod)(1)]^+$ and $[Rh(nbd)(1)]^+$, only two olefinic proton signals are detected in the temperature range 298–183 K, indicating that the protons H$^1$ and H$^2$, as well as protons H$^3$ and H$^4$, are isochronous at any temperature. In contrast, for $[Rh(cod)(2)]^+$, the four olefinic protons are non-equivalent at 298 K as they appear as four 1:1:1:1, somewhat broad, resonances which sharpen on cooling. For $[Rh(nbd)(2)]^+$, the two sharp signals of the olefinic protons at ambient temperature split into four 1:1:1:1 distinct resonances at 183 K. Such a dynamic behaviour can be rationalised by taking into account the possible conformers **A** and **A′**, which arise from the non-coplanarity of the chelating iminophosphines with the N–Rh–P coordination plane (Fig. 1), and their interconversion through a P–N ring inversion analogous to that described for iminophosphine–palladium derivatives [5]. The rate of this conformational change is affected markedly by the steric requirements of both the N–R substituent and the chelating diolefin.



R = C$_6$H$_3$($i$-Pr)$_2$-2,6    **:1**      [Rh(cod)(**1**)]BF$_4$; [Rh(nbd)(**1**)]BF$_4$

R = CMe$_3$          **:2**      [Rh(cod)(**2**)]BF$_4$; [Rh(nbd)(**2**)]BF$_4$

R = (R)-bornyl      **:3**      [Rh(cod)(**3**)]BF$_4$; [Rh(nbd)(**3**)]BF$_4$

[ (R)-bornyl = *endo*-(1R)-1,7,7,-trimethylbicyclo[2.2.1]hept-2-yl]

Scheme 1.

Table 1
Selected $^1$H $^a$ and $^{31}$P-{$^1$H} $^b$ NMR data

| Complex | Iminophosphine protons | | $^{31}$P resonances | | |
|---|---|---|---|---|---|
| | N=C$H$ | Other signals | H$^1$, H$^2$ | H$^3$, H$^4$ | |
| [Rh(cod)(**1**)]BF$_4$ | 8.01 d (2.7) $^b$ | 3.16 spt [C$H$(CH$_3$)$_2$]; 1.38 d, 0.74 d [CH(C$H_3$)$_2$] (6.9) $^c$ (6.7) $^c$ | 4.62 m | 3.82 m | 35.21 d (154.4) $^e$ |
| | | | 4.48 m $^d$ | 3.68 m $^d$ | |
| [Rh(nbd)(**1**)]BF$_4$ | 8.03 d (3.0) $^b$ | 3.13 spt [C$H$(CH$_3$)$_2$]; 1.46 d, 0.80 d [CH(C$H_3$)$_2$] (6.9) $^c$ (6.3) $^c$ | 4.60 s | 3.90 s | 32.70 d (170.2) $^e$ |
| [Rh(cod)(**2**)]BF$_4$ | 8.16 d (2.2) $^b$ | 1.28 s [C(CH$_3$)$_3$] | 5.50 s (br), 5.33 s (br) | 4.47 s (br), 3.78 s (br) | 32.87 d (152.9) $^e$ |
| [Rh(nbd)(**2**)]BF$_4$ | 8.04 s | 1.22 s [C(CH$_3$)$_3$] | 5.68 s | 4.01 s | 36.49 d (170.2) $^e$ |
| | | | 5.82 s $^d$, 5.58 s $^d$ | 4.08 s $^d$, 3.54 s $^d$ | |
| [Rh(cod)(**3**)]BF$_4$ | 8.22 s | 3.96 m [NC$H$]; 1.04 s [C$H_3$]; 0.94 s [C$H_3$], 0.79 s [C$H_3$] | 5.43 m, 5.16 m | 3.78 m, 3.63 m | 34.07 d (155.1) $^e$ |
| [Rh(cod)(**3**)]ClO$_4$ $^f$ | 8.31 s | 3.95 m [NC$H$]; 1.02 s [C$H_3$]; 0.91 s [C$H_3$], 0.77 s [C$H_3$] | 5.44 m, 5.23 m | 3.70 m, 3.55 m | 30.24 d (153.2) $^e$ |
| [Rh(nbd)(**3**)]BF$_4$ | 8.14 d (2.5) $^b$ | 3.84 m [NC$H$]; 1.09 s [C$H_3$]; 0.99 s [C$H_3$], 0.83 s [C$H_3$] | 5.57 s, 5.28 s | 4.06s, 3.71 s | 35.98 d (170.5) $^e$ |

$^a$ In CD$_2$Cl$_2$ at 298 K unless otherwise stated; satisfactory integration values were obtained; coupling constants in Hz; s, singlet; d, doublet; spt, septet; m, multiplet; see Scheme 1 for olefinic protons numbering.
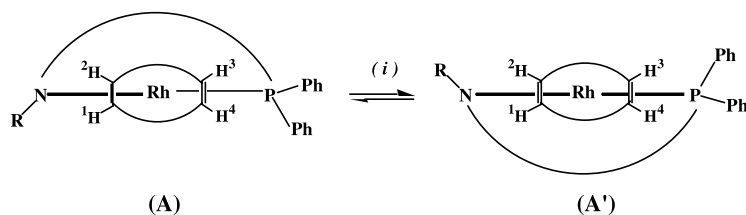$^b$ $J$(PH).
$^c$ $J$(HH).
$^d$ At 183 K.
$^e$ $J$(RhP).
$^f$ In CDCl$_3$.



Fig. 1. Side view from the diolefin ligand toward the Rh atom for the conformers of the complexes [Rh($\eta^2$,$\eta^2$-diolefin)(P–N)]$^+$. The curved line joining the N and P atoms represents the =CHC$_6$H$_4$– unit lying below or above the N–Rh–P plane: (i) interconversion through the chelate ring inversion of the P–N ligand.

When the ring inversion is fast (on the NMR time scale) a time-averaged plane of symmetry is generated in the N–Rh–P coordination plane, which brings about the equivalence of proton H$^1$ with H$^2$ and of proton H$^3$ with H$^4$. This is the case of complexes [Rh(cod)(**1**)]$^+$ and [Rh(nbd)(**1**)]$^+$ throughout the temperature range explored. In these compounds, the N–C$_6$H$_3$($i$-Pr)$_2$-2,6 moiety can minimise the steric interaction with the $cis$-CH$^1$=CH$^2$ olefinic unit by assuming a phenyl ring orientation almost perpendicular to the coordination plane. Such orientation is indeed supported by the shielding of the H$^1$ and H$^2$ protons due to the anisotropic effect of the phenyl ring current, and by the lack of free rotation around the N–C$_{phenyl}$ bond. In [Rh(cod)(**1**)]$^+$ and [Rh(nbd)(**1**)]$^+$ the H$^1$ and H$^2$ protons resonate at ca. 4.60

ppm, whereas the corresponding protons in the other complexes are found at lower field in the range 5.68–5.16 ppm. On the other hand, the hindered rotation is evidenced by the number of the CHMe$_2$ signals in the $^1$H-NMR spectra (see Table 1) which show the presence of two non-equivalent methyl groups within each of the mutually equivalent 2,6-isopropyl substituents.

The ring inversion rate decreases considerably upon introducing a bulky CMe$_3$ group as the imino nitrogen substituent in the complexes [Rh(nbd)(**2**)]$^+$ and [Rh(cod)(**2**)]$^+$. In the latter compound, containing also the more sterically demanding 1,5-cyclooctadiene ligand, the rate is reduced to such an extent that the H$^1$ and H$^2$ protons (as well as H$^3$ and H$^4$) are no longer equivalent even at ambient temperature. In this case,
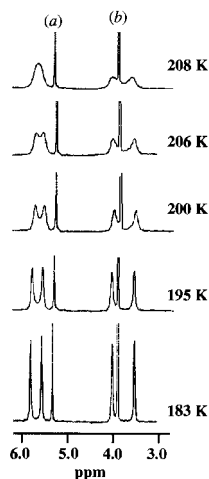
Fig. 2. Low temperature $^1$H-NMR spectra of [Rh(nbd)(**2**)]BF$_4$ in CD$_2$Cl$_2$ in the range 3.0–6.0 ppm: (a) solvent signal; (b) nbd (1)H and (4)H protons signal.

four 1:1:1:1 olefinic proton signals are observed for both the enantiomeric conformers **A** and **A′** which are not distinguishable under our experimental conditions. For [Rh(nbd)(**2**)]$^+$ containing a chelate diolefin of smaller size, the inversion rate is relatively high at ambient temperature, but decreases at lower temperatures. The spectral changes in the temperature range 208–183 K are shown in Fig. 2.

As can be seen, the resonances at 5.82 and 5.58 ppm (183 K) of the olefinic protons H$^1$, H$^2$ coalesce at 208 K. A line-shape analysis of the signals [13] yields the following activation parameters for the dynamic process: $\Delta H^{\#} = 28.5$ kJ mol$^{-1}$, $\Delta S^{\#} = -60.3$ J K$^{-1}$ mol$^{-1}$, and $\Delta G^{\#} = 41.0$ kJ mol$^{-1}$. The spectra at higher temperatures (not reported in Fig. 2) show a

coalescence of the resonances at 4.08 and 3.54 ppm (olefinic protons H$^3$, H$^4$) at 228 K, from which a $\Delta G^{\#}$ value of 43.9 kJ mol$^{-1}$ can be estimated [13]. The negative activation entropy suggests a transition state with reduced degrees of freedom, which can be achieved without any breaking of the rhodium–ligand bonds when the six-membered ring of the chelating iminophosphine becomes coplanar with the N–Rh–P coordination plane. Comparable free energies of activation (34.3–39.3 kJ mol$^{-1}$) have been reported for the conformational change involving inversion of the iridium–diphosphine chelate ring in the complexes [Ir(cod)(L–L′)]$^+$ [L–L′ = 1,1′-bis(phosphino)ferrocene] [14].

For the complexes [Rh(cod)(**3**)]$^+$ and [Rh(nbd)(**3**)]$^+$ with a chiral N-(*R*)-bornyl group, the conformers **A** and **A′** are diasteromeric species. At ambient temperature, the $^1$H and $^{31}$P spectra show a single set of proton resonances for both the diolefin and the iminophosphine ligands, and a sharp $\delta$ ($^{31}$P) doublet (due to $^{103}$Rh coupling) for each cationic complex, independently of the counterion and solvent. No splitting of the signals occurs at lower temperatures. Only a progressive broadening of the phenyl proton resonances is observed when the temperature is lowered down to 183 K in CD$_2$Cl$_2$. These data are consistent with either the presence of one single diastereoisomer or with the two isomeric forms **A** and **A′** in fast exchange on the NMR time scale. That the latter is the case is shown by the 2D $^1$H-NMR ROESY spectra of [Rh(cod)(**3**)]$^+$ (as ClO$_4^-$ salt in CDCl$_3$ and as BF$_4^-$ salt in CD$_2$Cl$_2$) at ambient temperature. In both solvents, the same intra- and interligand NOEs are observed. However, their number is much higher than what would be expected for a single diastereoisomer, and is in agreement with the presence of both forms **A** and **A′** in fast interconver-
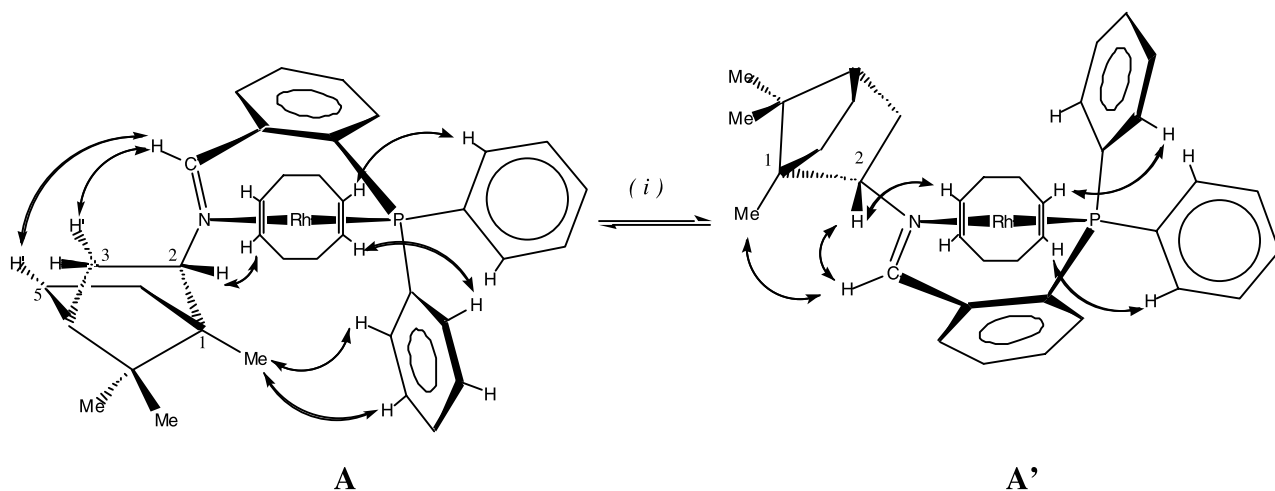


**A**                                                                          **A'**

Fig. 3. Side view from the 1,5-cyclooctadiene toward the Rh atom for the diastereoisomers of [Rh(cod)(**3**)]ClO$_4$, showing the contact NOEs observed in the 2D $^1$H-NMR ROESY spectrum in CDCl$_3$.
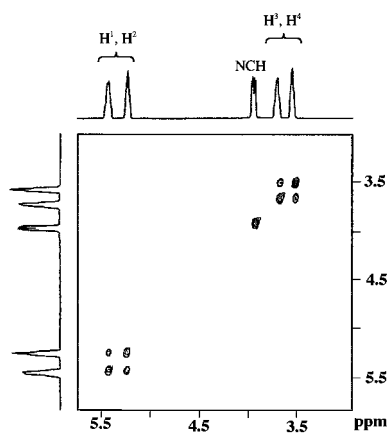
Fig. 4. Phase-sensitive 2D $^1$H-NMR ROESY spectrum of [Rh(cod)(3)]ClO$_4$ in the region of the olefinic proton signals. Only positive NOEs are shown.
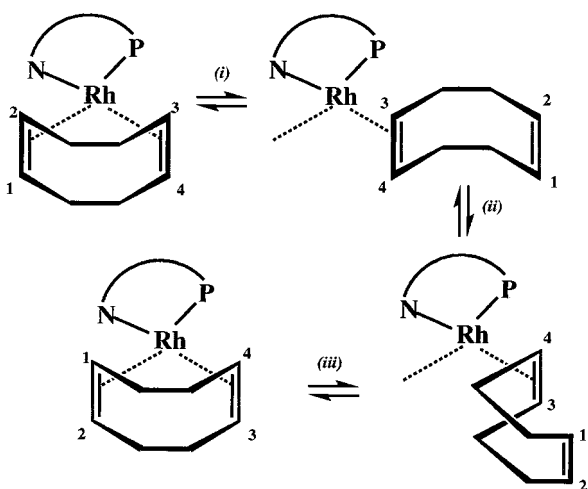


Scheme 2.

sion. As shown in Fig. 3 for the CDCl$_3$ spectrum, contact cross peaks are detected between the imino protons N=CH (at 8.31 ppm) and the (3)H′ and (5)H′ protons of the bornyl group (at 1.85 and 0.27 ppm, respectively), and between the bornyl (1)Me protons (at 1.02 ppm) and the *ortho* and *meta* protons of the axial P–Ph group (in the range 7.5–7.3 ppm) for isomer **A**, in addition to the NOEs N=C–H↔(2)H (at 3.95 ppm) and N=C–H↔(1)Me for isomer **A′**.

Furthermore, strong NOEs are also present between the bornyl (2)H proton and both the cod protons at 5.44 and 5.23 ppm, which confirm their assignment to the olefinic protons H$^1$, H$^2$ *trans* to phosphorus. Medium-to-strong NOEs are also observed between the PPh$_2$ *ortho* protons (in the range 7.4–7.2 ppm) and both the cod protons at 3.70 and 3.55 ppm, which confirms their assignment to the olefinic protons H$^3$, H$^4$ *trans* to nitrogen.

The 2D $^1$H-NMR ROESY spectrum of [Rh(cod)-(3)]$^+$ in the phase-sensitive mode shows exchange cross-peaks between the two olefinic protons *trans* to P and exchange cross-peaks between the two olefinic protons *trans* to N. No exchange cross-peaks involving the olefinic protons *trans* to P and those *trans* to N are present, as can be seen in Fig. 4.

These data indicate the occurrence of a slow dynamic process which selectively interconverts the two protons on the same HC=CH unit of the chelate cod ligand. This finding is unprecedented since in the molecular dynamics of the complexes [Rh(cod)(L–L′)]$^+$ (L–L′ = P,N-bidentate ligand) the only exchanges observed so far involve the olefinic protons *trans* to P with those *trans* to N, when L–L′ is an achiral ligand [11a], or the protons H$^1$ ⇌ H$^3$ and H$^2$ ⇌ H$^4$ when L–L′ is a chiral ligand [11b,12]. In these cases, the dynamic process was explained by a mechanism where the apparent rotation of the chelate cod ligand results from a P,N-ligand site exchange through initial rupture of the Rh–N bond. The stereochemical non-rigidity of the complex [Rh{Fe($\eta^5$-C$_5$H$_4$(2-C$_5$H$_4$N))($\eta^5$-C$_5$H$_4$PPh$_2$)}(cod)]PF$_6$ was also explained by a similar mechanism [15].

For the selective H$^1$ ⇌ H$^2$ and H$^2$ ⇌ H$^4$ exchanges observed for [Rh(cod)(3)]$^+$, we propose the mechanism of Scheme 2.

This mechanism involves (i) initial dissociation of the bond between rhodium and the CH$^1$=CH$^2$ olefinic unit (labilised by the high *trans* influence of the phosphine and also by steric interaction with the *cis*-N-(R)-bornyl group) with concomitant inversion of the olefin coordinating face in the Rh(CH$^3$=CH$^4$) bond; (ii) rotation of the $\eta^2$-cod ligand around the remaining rhodium–olefin bond axis; (iii) inversion of the flexible $\eta^2$-cod ligand configuration and re-association to form the chelate $\eta^2,\eta^2$-cod structure.

### 2.3. Diolefin exchange and displacement reactions

According to $^1$H-NMR spectra of the mixtures [Rh($\eta^2,\eta^2$-diolefin)(P–N)]$^+$/diolefin at room temperature, the exchange rate between the free and coordinated diolefin is slow, if any, on the NMR time scale. No appreciable broadening of the corresponding signals is in fact observed. However, the cod ligand in the complexes [Rh(cod)(P–N)]$^+$ is displaced rapidly and quantitatively by norbornadiene (Rh/nbd = 1:1.2 molar ratio, Eq. (2)):

$$[Rh(cod)(P-N)]^+ \xrightarrow[-\,cod]{+\,nbd} [Rh(nbd)(P-N)]^+ \qquad (2)$$
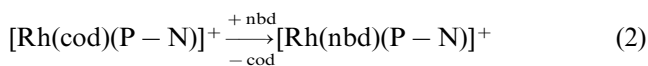
In contrast, no diolefin displacement takes place when the complexes [Rh(cod)(P–N)]$^+$ are treated with an excess of ethylene.

## 2.4. Theoretical calculations

In order to get more information about the preferred iminophosphine conformation and the steric interactions between the coordinated ligands, we have carried out a semi-empirical calculation on the cationic complexes $[Rh(nbd)(2)]^+$ and $[Rh(cod)(2)]^+$. In the most stable conformer of $[Rh(nbd)(2)]^+$ (enthalpy of formation = 394.1 kJ mol$^{-1}$) the P–N ligand assumes the coordination mode shown in Fig. 5, whereas in the most stable conformer of $[Rh(cod)(2)]^+$ (enthalpy of formation = 217.8 kJ mol$^{-1}$) the P–N coordination mode is shown in Fig. 6.

In these structures, which correspond to conformer **A** for $[Rh(nbd)(2)]^+$ and to conformer **A′** for $[Rh(cod)(2)]^+$ (see Fig. 1), the $=CHC_6H_4-$ unit lies out of the N–Rh–P coordination plane, whereas the N–CMe$_3$ group and one of the PPh$_2$ phenyl groups are



a : H•••H = 1.79 Å

b : H•••H = 2.89 Å

c : H•••H = 2.89 Å

Fig. 7. Perspective view parallel to the N–Rh–P plane for the most stable conformer of the molecule $[Rh(nbd)(2)]^+$. The $=CHC_6H_4-$ unit has been omitted for clarity.



Rh-N = 1.98 Å          N-R̂h-P = 84.6°

Rh-P = 2.34 Å
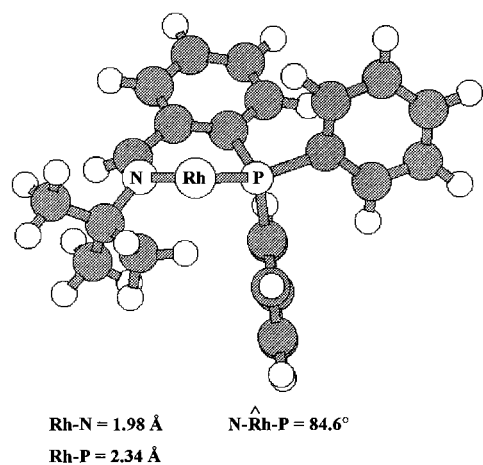
Fig. 5. Perspective view parallel to the N–Rh–P plane for the most stable conformer of the molecule $[Rh(nbd)(2)]^+$. The diolefin ligand has been omitted for clarity.



a : H•••H = 1.74 Å

b : H•••H = 2.89 Å

c : H•••H = 3.83 Å

Fig. 8. Perspective view parallel to the N–Rh–P plane for the most stable conformer of the molecule $[Rh(cod)(2)]^+$. The $=CHC_6H_4-$ unit has been omitted for clarity.



Rh-N = 1.98 Å          N-R̂h-P = 83.7°

Rh-P = 2.34 Å
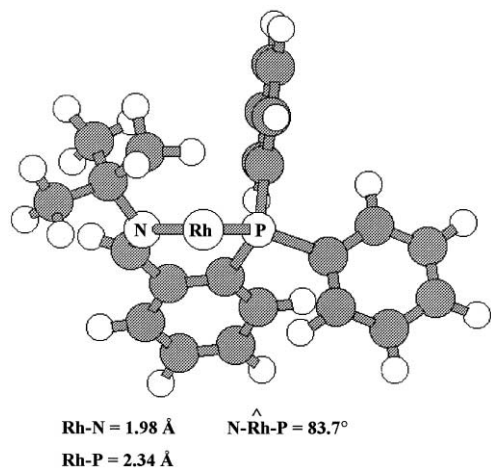
Fig. 6. Perspective view parallel to the N–Rh–P plane for the most stable conformer of the molecule $[Rh(cod)(2)]^+$. The diolefin ligand has been omitted for clarity.
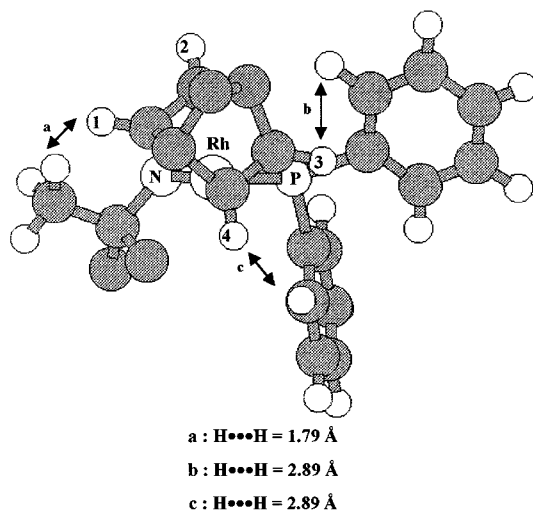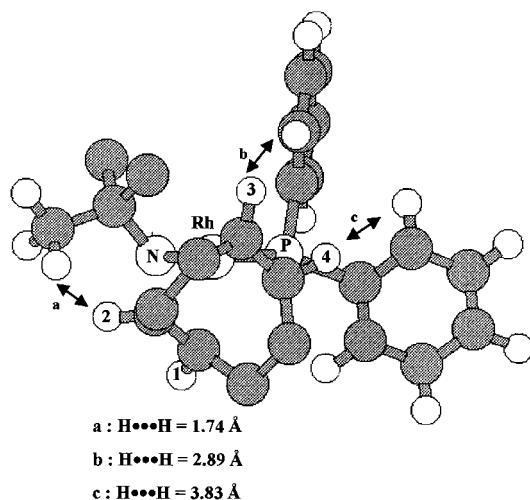
on the opposite side. Interestingly, the calculations yield P–N conformations for the isolated molecules which are in a good agreement with those observed in the solid state for palladium complexes containing related iminophosphine ligands [5].

The coordination of the diolefin ligands is characterised by a large distortion from their idealised position in square-planar complexes, as can be seen in Fig. 7 for $[Rh(nbd)(2)]^+$ and in Fig. 8 for $[Rh(cod)(2)]^+$.

Such a distortion is essentially due to the steric interaction with the N–CMe$_3$ group, as can be inferred from the short distances between the olefinic protons *trans* to phosphorus and the protons of the CMe$_3$ group. The shortest interligand contacts are actually observed between one of the CMe$_3$ protons and the H$^1$

Table 2
Elemental analysis and selected IR data

| Complex | Analysis [a] | | | IR bands [b] | |
|---|---|---|---|---|---|
| | C | H | N | $\nu$(C=N) | $\nu$(B–F) |
| [Rh(cod)(**1**)]BF$_4$ | 62.8 (62.67) | 5.9 (5.93) | 1.9 (1.87) | 1602 ms | 1054 vs |
| [Rh(nbd)(**1**)]BF$_4$ | 61.7 (62.40) | 5.5 (5.51) | 1.9 (1.91) | 1601 ms | 1053 vs |
| [Rh(cod)(**2**)]BF$_4$ | 57.4 (57.87) | 5.6 (5.64) | 2.2 (2.18) | 1608 ms | 1054 vs |
| [Rh(nbd)(**2**)]BF$_4$ | 56.9 (57.44) | 5.1 (5.14) | 2.2 (2.23) | 1610 ms | 1061 vs |
| [Rh(cod)(**3**)]BF$_4$ | 61.1 (61.43) | 6.0 (6.13) | 1.9 (1.94) | 1621 ms | 1069 vs |
| [Rh(cod)(**3**)]ClO$_4$ | 60.1 (60.27) | 6.0 (6.02) | 1.9 (1.90) | 1617 ms | 1089 vs [c] |
| Rh(nbd)(**3**)]BF$_4$ | 60.7 (61.12) | 5.6 (5.70) | 1.9 (1.98) | 1623 ms | 1064 vs |

[a] Calculated values in parenthesis.
[b] As nujol mulls.
[c] $\nu$(Cl–O).

olefinic proton of [Rh(nbd)(**2**)]$^+$ (1.79 Å) or the H$^2$ olefinic proton of [Rh(cod)(**2**)]$^+$ (1.74 Å). As a consequence, both the olefinic carbons *trans* to phosphorus are shifted above or below the N–Rh–P plane. Some distortion of the coordinated diolefin has been observed in the X-ray structural studies of complexes [Rh($\eta^2,\eta^2$-diolefin)(L–L′)]$^+$ (L–L′ = P,N- and P,P-bidentate ligand) [11b,12,16].

The presence of distorted diolefins and, consequently, of weak rhodium–olefin bonds is likely to be responsible for the instability of the complexes studied toward traces of water in solution.

The changes in the enthalpy content during the chelate ring inversion of the P–N ligand were also estimated. The enthalpy reaches a maximum value when the six-membered chelate ring is coplanar with the N–Rh–P coordination plane. The enthalpy increase is $\Delta H = 20.3$ kJ mol$^{-1}$ for [Rh(nbd)(**2**)]$^+$ and $\Delta H = 114.7$ kJ mol$^{-1}$ for [Rh(cod)(**2**)]$^+$. The calculated $\Delta H$ value for the former complex compares well with the activation enthalpy of 28.5 kJ mol$^{-1}$ measured in CD$_2$Cl$_2$ solution at 208 K. On the other hand, the large difference in $\Delta H$ values for the two compounds is in accord with the different rates of ring inversion observed in solution.

When the inversion process is complete, the complex [Rh(nbd)(**2**)]$^+$ assumes the structure of conformer **A′** (with an enthalpy of formation of 394.2 kJ mol$^{-1}$) and the complex [Rh(cod)(**2**)]$^+$ assumes the structure of conformer **A** (with an enthalpy of formation of 219.1 kJ mol$^{-1}$). As expected for enantiomeric pairs, these enthalpy values are very close to those of the starting conformers **A** and **A′**.

From the enthalpies of formation of the free diolefins, calculated by using the same semi-empirical method for the most stable conformer of 1,5-cyclooctadiene (69.5 kJ mol$^{-1}$) and for norbornadiene (245.0 kJ mol$^{-1}$), and from the enthalpies of formation of the most stable conformers of [Rh(nbd)(**2**)]$^+$ and [Rh(cod)(**2**)]$^+$ a $\Delta H$ value of 0.8 kJ mol$^{-1}$ can be

estimated for reaction 2 involving the isolated molecules. Since solvation effects are expected to play a minor role for structurally related molecules, the small $\Delta H$ value indicates that reaction 2 in solution is essentially entropy driven. This is indirectly confirmed by the lack of diolefin displacement when an excess of ethylene is added to a solution of [Rh(cod)(**2**)]$^+$.

## 3. Experimental

### 3.1. General

All manipulations were carried out under a dry N$_2$ atmosphere. Diethyl ether was distilled from Na/benzophenone, and CH$_2$Cl$_2$ from LiAlH$_4$. All other chemicals and solvents were reagent grade and were used without further purification. The iminophosphines [10] and the complexes [Rh($\mu$-Cl)(cod)]$_2$ [17] and [Rh($\eta^2,\eta^2$-diolefin)$_2$]BF$_4$ [18] were prepared by literature methods. The $^1$H- and $^{31}$P{$^1$H}-NMR spectra were recorded on a Bruker AM400 spectrometer operating at 400.13 and 161.98 MHz, respectively. Chemical shifts (ppm) are given relative to Me$_4$Si ($^1$H-NMR) and 85% H$_3$PO$_4$ ($^{31}$P-NMR). The 2D $^1$H-NMR ROESY spectra were obtained in the phase-sensitive mode as described elsewhere [5,10]. The IR spectra of solid samples were recorded in the range 4000–200 cm$^{-1}$ on a Perkin–Elmer 983 G instrument with CsI windows.

### 3.2. Preparation of [Rh($\eta^2,\eta^2$-diolefin)(P–N)]BF$_4$

The iminophosphine (**1**–**3**) (0.5 mmol) was added to a solution of [Rh($\eta^2,\eta^2$-diolefin)$_2$]BF$_4$ (0.5 mmol) in CH$_2$Cl$_2$ (30 cm$^3$). After standing for 1 h at room temperature (r.t.), the red–orange solution was concentrated at reduced pressure, and diluted with Et$_2$O to precipitate the products as yellow–orange microcrystalline solids. The yields were in the range 80–93%, based on the theoretical amount. The complexes are

uni-univalent electrolytes in $CH_2Cl_2$, with molar conductivity values in the range $52-55$ $\Omega^{-1}$ $cm^2$ $mol^{-1}$ for $1 \times 10^{-3}$ mol $dm^{-3}$ solutions at 25 °C. The elemental analysis and some selected IR bands are reported in Table 2.

### 3.3. Preparation of [Rh(cod)(3)]ClO₄

The iminophosphine **3** (0.170 g, 0.4 mmol) was added to a solution of $[Rh(\mu\text{-Cl})(cod)]_2$ (0.099 g, 0.2 mmol) in $CH_2Cl_2$ (20 $cm^3$). Upon addition of an excess $NaClO_4 \cdot H_2O$ (0.112 g, 0.8 mmol) dissolved in $Me_2CO$ (20 $cm^3$), an immediate precipitation of NaCl took place. The solvents were evaporated to dryness and the solid residue was extracted with $CH_2Cl_2$ (40 $cm^3$). After filtration, the solution was concentrated to small volume and diluted with $Et_2O$ to give an orange solid. The product was further purified by reprecipitation from the same solvent mixture (yield, 0.236 g, 80.2%; molar conductivity, 46.2 $\Omega^{-1}$ $cm^2$ $mol^{-1}$ for a $1 \times 10^{-3}$ mol $dm^{-3}$ solution at 25 °C).

### 3.4. Computations

Semi-empirical calculations were carried out with PM3 method [19] using the HYPERCHEM program [20]. Geometric optimisations were terminated when the energy difference among successive iterations was lower than $4.184 \times 10^{-3}$ kJ $mol^{-1}$. Computations were performed using as initial values the structural parameters from crystallographic data of the complexes $[Rh(\eta^2,\eta^2\text{-diolefin})(L-L')]^+$ (diolefin = nbd, cod; L–L′ = P,N- and P,P-bidentate ligand) [11b,12,14–16,21].

### References

[1] E. Shirakawa, T. Hiyama, J. Organomet. Chem. 576 (1999) 169 (and references therein).

[2] E.K. van den Beuken, W.J.J. Smeets, A.L. Spek, B.L. Feringa, J. Chem. Soc. Chem. Commun. (1998) 223.

[3] K.R. Reddy, C.L. Chen, Y.H. Liu, S.M. Peng, J.T. Chen, S.T. Liu, Organometallics 18 (1999) 2574.

[4] (a) K. Fugami, Y. Mishiba, S. Hagiwara, D. Koyama, M. Kameyama, M. Kosugi, Synlett (2000) 553;
(b) H.-Y. Jang, H. Seo, J.W. Han, Y.K. Chung, Tetrahedron Lett. 41 (2000) 5083.

[5] (a) B. Crociani, S. Antonaroli, G. Bandoli, L. Canovese, F. Visentin, P. Uguagliati, Organometallics 18 (1999) 1137;
(b) G. Bandoli, A. Dolmella, L. Crociani, S. Antonaroli, B. Crociani, Transition Met. Chem. 25 (2000) 17.

[6] I.D. Kostas, C.G. Screttas, J. Organomet. Chem. 585 (1999) 1.

[7] (a) M. Mc Carty, M.W. Hooper, J.P. Guiry, J. Chem. Soc. Chem. Commun. (2000) 1333;
(b) S.U. Son, H.-Y. Jang, J.W. Han, I.S. Lee, Y.K. Chung, Tetrahedron: Asymmetry 10 (1999) 347.

[8] H. Yang, H. Gao, R.J. Angelici, Organometallics 19 (2000) 622.

[9] C.A. Gilardi, S. Midollini, S. Moneti, A. Orlandini, G. Scapacci, J. Chem. Soc. Dalton Trans. (1992) 3371.

[10] (a) S. Antonaroli, B. Crociani, J. Organomet. Chem. 560 (1998) 137;
(b) B. Crociani, S. Antonaroli, L. Canovese, F. Visentin, P. Uguagliati, Inorg. Chim. Acta 315 (2001) 172.

[11] (a) H. Yang, N. Lugan, R. Mathieu, Organometallics 16 (1997) 2089 (and references therein);
(b) H. Berger, R. Nesper, P.S. Pregosin, H. Rüegger, M. Wörle, Helv. Chim. Acta 76 (1993) 1520.

[12] M. Valentini, K. Selvakumar, M. Wörle, P.S. Pregosin, J. Organomet. Chem. 587 (1999) 244.

[13] B. Testa, Principles of Organic Stereochemistry, Marcel Dekker, New York, 1979.

[14] A.G. Avent, R.B. Bedford, P.A. Chaloner, S.Z. Dewa, P.B. Hitchcock, J. Chem. Soc. Dalton Trans. (1996) 4633.

[15] T. Yoshida, K. Tani, T. Yamagata, Y. Tatsuno, T. Saito, J. Chem. Soc. Chem. Commun. (1990) 292.

[16] (a) M.J. Burk, J.E. Feaster, R.L. Harlow, Tetrahedron: Asymmetry 2 (1991) 569;
(b) M.J. Burk, J.E. Feaster, W.A. Nugent, R.L. Harlow, J. Am. Chem. Soc. 115 (1993) 10125.

[17] G. Giordano, R.H. Crabtree, Inorg. Synth. 28 (1990) 88.

[18] T.G. Schenk, J.M. Downes, C.R.C. Milne, P.B. Mackenzie, H. Boucher, J. Whelan, B. Bosnich, Inorg. Chem. 24 (1985) 2334.

[19] J.J.P. Stewart, J. Comput. Chem. 10 (1989) 209.

[20] HYPERCHEM Release 6.02 for Windows, Hypercube Inc., 2000.

[21] (a) W.R. Cullen, F.W.B. Einstein, C.-H. Huang, A.C. Willis, E.-S. Yeh, J. Am. Chem. Soc. 102 (1980) 988;
(b) J. Bokos, I. Tóth, B. Heil, G. Szalontai, L. Párkányi, V. Fülöp, J. Organomet. Chem. 370 (1989) 263;
(c) X. Zhang, K. Mashima, K. Koyano, N. Sayo, H. Kumobayashi, S. Akugatawa, H. Takoya, J. Chem. Soc. Perkin Trans. 1 (1994) 2309;
(d) A. Marinetti, C. Le Menn, L. Ricard, Organometallics 14 (1995) 4983;
(e) N. Feiken, P.S. Pregosin, G. Trabesinger, Organometallics 17 (1998) 4510.